Performance evaluation of T-shaped tree heat exchanger with rectangular channels with constant height

Ventsislav Zimparov[a], Milcho Angelov[b], Plamen Bonev[a], Plamen Penchev[a]

[a]Department of Mechanical Engineering, Technical University of Gabrovo, 4 "Hadji Dimitar Str." 5300 Gabrovo, Bulgaria, e-mail ventsi.zimparov@gmail.com
[b]Technical Faculty, University of Food Technologies, Plovdiv, Bulgaria
Center of competence "Smart Mechatronics, Eco- and Energy Saving Systems and Technologies".

Abstract:

This study evaluates the performance characteristics of a heat exchanger with a T-shaped tree flow configuration with a rectangular shape and constant height *H* of the channels. The flow is laminar and fully developed with constant physical properties. The boundary condition is the fixed temperature of the channel wall. The fractal design is selected with the ratios $L_{i+1}/L_i = 2^{1/2}$ for the lengths and $W_{i+1}/W_i = 2^{1/3}$ for the widths of the channels. The width of the terminal channels W_o is optional, and the ratios $W_o^* = W_o/H = 1$, 1.618 (golden ratio), and 2 have been selected for investigation. The criteria for performance evaluation are the variations of the increase in the heat flow ratio $q_t^+ > 1$ and the decrease in the augmentation entropy generation number $N_{sa} < 1$ with the dimensionless mass flow rate *M*, width ratio W_o^*, *B,* and complexity *n*. The performance evaluation criterion N_s^+ has been introduced as a general criterion to define the most beneficial complexity and working parameters of the tree-shaped design only for these regions of *M* where both criteria $q_t^+ > 1$ and $N_{sa} < 1$ are fulfilled simultaneously. The obtained results showed that the efficiency of the T-shaped heat exchanger increases when *B* decreases, whereas W_o^* the complexity *n* increases.

Keywords:

T-shaped tree; Rectangular shape; Constant height of the channels, Maximum benefit; Performance evaluation criteria.

1. Introduction

The dendritic heat exchangers are a distinctly new direction for the development of heat exchanger architectures that arose at the beginning of this century, apart from the classical heat exchanger design methods [1]. The constructal theory revealed a great potential to reduce the pressure drop and wall temperature and increase the thermal efficiency of the fractal tree-like nets compared with classical heat exchangers that use parallel channel networks [2-4]. Since then, many experimental and numerical studies have been reported [5]. The performance of balanced two-stream counterflow [6] or parallel flow [7] heat exchangers as a tree network has been studied theoretically and experimentally [8]. The optimization of the T- and Y-shaped assemblies of ducts has also been presented [9,10]. The detailed literature review shows that most of the tree-shaped heat exchangers studied considered constant channel depth throughout the fractal-like network [2-4, 11,12]. The effects of the continuously varying channel depth on the overall performance of the tree-shaped HEx are rarely reported [13-15].

1.1. Objective

The objective of this study is to define the maximum performance of a heat exchanger that has a T-shaped tree flow configuration and a rectangular shape, with channels of constant height. To solve this task, first of all, we have to realize and answer the next two questions:

(i) What does a maximum benefit for a T-shaped tree flow configuration mean?

(ii) Is there any limit to the complexity n (number of branching levels) when the tree evolves?

In this paper, we demonstrate the usefulness of two criteria, similar to the criteria used in the cases FG-1a, and FG-1b [16], namely, augmentation entropy generation number N_{sa} and q_t^+ when the thermal characteristic of a dendritic T-shaped heat exchanger has been compared with that of a serpentine structure. The objective of the first case (FG-1a) is to obtain a maximum increase of the heat duty, $q_t^+ > 1$, whereas the objective of the second case (FG-1b) is to obtain a maximum reduction of the driving temperature difference $\Delta T_m^* < 1$.

The constraints of both cases are defined as follows: fixed inlet flow and wall temperatures, mass flow rate, heat transfer surface area in an allocated area, and $N_{sa} \le 1$. This paper addresses new insight into the problem studied previously by Zimparov et al. [15] with corrections, developments, supplements, and new ideas drawn. The precise problem formulation is explained next.

2. Detailed analysis of complex heat exchanger configurations

2.1. Comparison between T-shaped tree with serpentine structure heat exchangers

Consider the case of incompressible flow through the T-shaped structure and tree-shaped streams distributed over a rectangular area, Fig. 1, upon the following assumptions: (1) the flow is laminar and fully developed with constant physical properties; (2) the effect of bifurcations on pressure drop is negligible. The constraints are fixed heat transfer surface area of the channels $A_w = const$ and the allocated area, $A = const$. The boundary condition of the channel wall is a constant temperature $T_w = const$.

For the selected design configuration, the lengths obey the rule $L_i = 2^{i/2} L_o$ and $D_{h,i} = 2^{i/3} D_{h,o}$. In this case, the numbers of flow rates are ordered as:

$$n_i = 2^{n-i}, \qquad \dot{m}_i = 2^i \dot{m}_o, \qquad \dot{m} = \dot{m}_n = 2^n \dot{m}_o \qquad (i = 0,1,.....n) \tag{1}$$

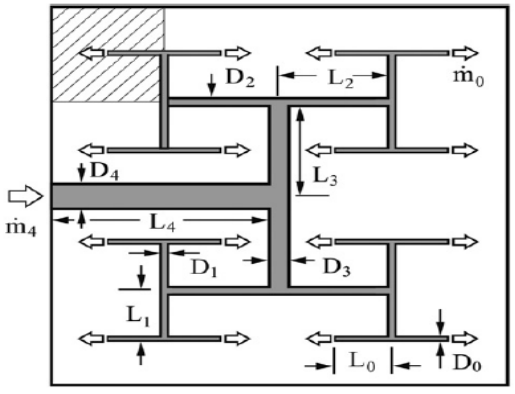

Figure 1. Flow of tree-shaped streams distributed over a rectangular area

with $D_{h,i} = \dfrac{2^{(i+3)/3} W_o^*}{\left(2^{i/3} W_o^* + 1\right)} H$, where $W_o^* = \dfrac{W_o}{H}$. The total area covered by the largest construct (the n^{th} construct) is $A = 2^n (2L_o)^2 = 2^{n+2} L_o^2$, or

$$L_o = \frac{A^{1/2}}{2^{(n+2)/2}} \,. \tag{2}$$

The total tube heat transfer surface area is

$$A_w = \sum_{i=0}^{n} n_i p_i L_i = \sum_{i=o}^{n} n_i \chi_i D_{h,i} L_i = 2^{(n-2)/2} A^{1/2} W_o^* H \sum_{i=o}^{n} \frac{2^{-i/2} \chi_i}{\left(2^{i/3} W_o^* + 1\right)} \tag{3}$$

with

$$\chi_i = \frac{\left(2^{i/3} W_o^* + 1\right)^2}{2^{i/3} W_o^*} \quad . \tag{4}$$

The mathematical model developed in [10,15] has been adapted to the case studied. The results obtained (in dimensionless forms) for the total heat flow $\tilde{q}_{tot}$ and entropy generation rate $\tilde{S}_{gen}$ are as follows:

$$\tilde{q}_{tot} = \frac{\dot{q}_{tot}}{k_f A^{1/2} T_{in}} = M\left(T^* - 1\right)\left\{\left[1 - \exp\left(-\chi_i Nu_i \frac{2^{(n-2)/2}}{M}\right)\right] + S_1\right\} \tag{5a}$$

with

$$S_1 = \sum_{i=1}^{n}\left\{\exp\left(-\sum_{k=0}^{k=i-1} \chi_i Nu_i \frac{2^{(n-k-2)/2}}{M}\right)\left[1 - \exp\left(-\chi_i Nu_i \frac{2^{(n-i-2)/2}}{M}\right)\right]\right\} \tag{5b}$$

$$\tilde{S}_{gen} = M\left(T^* - 1\right)^2 \left\{\exp\left(-\chi_i Nu_i \frac{2^{(n-2)/2}}{M}\right)\left[1 - \exp\left(-\chi_i Nu_i \frac{2^{(n-2)/2}}{M}\right)\right] + S_2\right\} + \\ + \frac{BM^2}{2^{(n+4)/2}(W_o^*)^4} \times \sum_{i=o}^{n} 2^{5i/6}(2^{i/3} W_o^* + 1)^4 \frac{Po_i}{\chi_i} \tag{6a}$$

with

$$S_2 = \sum_{i=1}^{n}\left\{\left[\exp\left(-\sum_{k=0}^{k=i-1} \chi_i Nu_i \frac{2^{(n-k-2)/2}}{M}\right)\right]^2 \exp\left(-\chi_i Nu_i \frac{2^{(n-i-2)/2}}{M}\right) \times \right. \\ \left. \times\left[1 - \exp\left(-\chi_i Nu_i \frac{2^{(n-i-2)/2}}{M}\right)\right]\right\} \tag{6b}$$

and

$$M = \frac{\dot{m} c_p}{k_f A^{1/2}}, \qquad B = \frac{A^{3/2} \nu k_f}{H^4 T_w \rho c_p^2} \tag{6c}$$

$$Po_i \equiv (f\,\mathrm{Re})_i = 24\left(1 - 1.3553\alpha_{i,*} + 1.9467\alpha_{i,*}^2 - 1.7012\alpha_{i,*}^3 + 0.9564_{i,*}^4 - 0.2537\alpha_{i,*}^5\right) \tag{6d}$$

$$Nu_i = 7.541\left(1 - 2.61\alpha_{i,*} + 4.97\alpha_{i,*}^2 - 5.119\alpha_{i,*}^3 + 2.702\alpha_{i,*}^4 - 0.548\alpha_{i,*}^5\right) \tag{6e}$$

$$\alpha_{i,*} = \frac{2b}{2a} = \frac{H}{W_i} = 2^{-i/3}\left(W_o^*\right)^{-1}. \tag{6f}$$

The definition of Po_i and Nu_i, Eqs. (6d-6f), have been derived from [18].

2.2. Performance evaluation criteria

When the complexity is $n=0$, the tree-shaped heat exchanger transforms into either a one-tube or serpentine structure. To assess the benefits of replacing the serpentine heat exchanger configuration with the tree-shaped structure heat exchanger, the following ratios can be defined as related to the overall heat flow and entropy generation, as

a) The ratio q_t^+ is defined as the total heat flow of the tree-shaped heat exchanger with complexity n compared with a tree-shaped heat exchanger with complexity $n=0$

$$q_t^+ = \frac{\tilde{q}_{tot,n}}{\tilde{q}_{tot,n=0}}. \tag{7}$$

b) The augmentation entropy generation number, N_{sa}, defined as a ratio between the total entropy generation of a tree-shaped heat exchanger with complexity *n* compared with the total entropy generation of a tree-shaped heat exchanger with complexity $n=0$

$$N_{sa} = \frac{\tilde{S}_{gen,n}}{\tilde{S}_{gen,n=0}}. \tag{8}$$

c) Criterion for thermal efficiency and maximum performance, N_s^+

$$N_s^+ = \frac{N_{sa}}{q_t^+} \tag{9}$$

which applies only when the following two goals are achieved namely: $q_t^+ \geq 1$ and $N_{sa} \leq 1$.

3. New results and discussion

3.1. Comparison between T-shaped tree exchanger and a serpentine structure heat exchanger

In this section, we made a comparison between the thermal performance characteristics of two tree-shaped constructs with design $D_{h,i} = 2^{i/3} D_{h,o}$ and $L_i = 2^{i/2} L_o$ according to the PEC defined by Eqs. (7-9) to select the more beneficial tree-shaped structure. As seen from Eqs. (5a) and (6a) the ratio q_t^+ depends on the mass flow rate *M* and complexity *n*, whereas the augmentation entropy generation number depends on *M, n* and *B*.

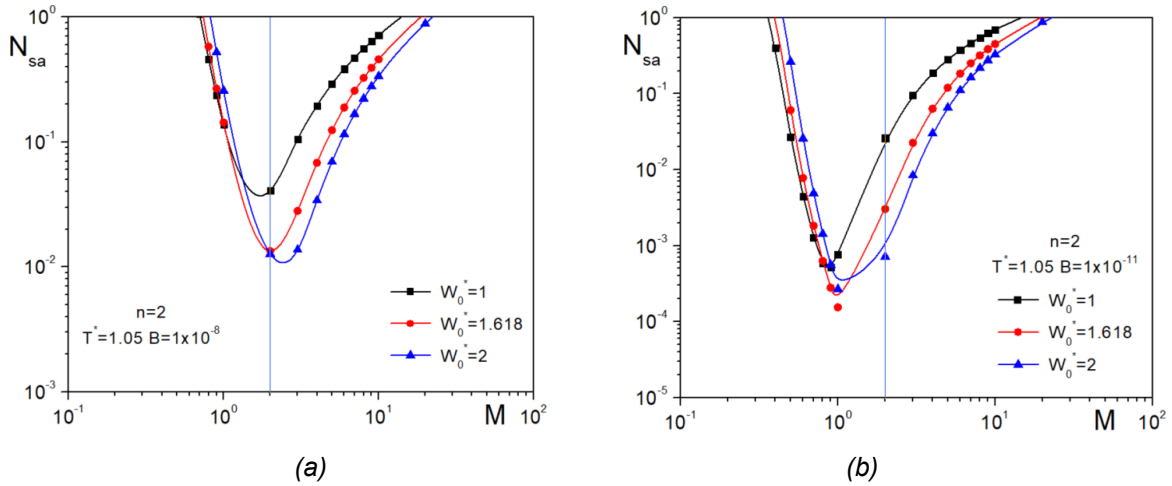

Figure 2. The variation of N_{sa} *with B, M, and* W_o^* ($n=2$, $T^*=1.05$)

Figure 2 represents the variation of the augmentation entropy generation number N_{sa} (constrained from the second law) with the dimensionless mass flow rate M and the complex B ($n=2$ and $T^*=1.05$). The preliminary calculations revealed that the imposed constrain $N_{sa}\le 1$ fulfills if $B<10^{-6}$. It means that this tree-shaped design does not carry any benefit, if $B>10^{-6}$. As seen from Fig. 2, several important conclusions can be derived:

(a) when W_o^* increases N_{sa} decreases;

(b) when *B* decreases, $B<10^{-6}$, N_{sa} also decreases;

(c) The curves N_{sa} vs. *M* possess a minimum, and this minimum moves to the left (to smaller *M*).

(d) The most important result is the maximum value of *M*, limiting the benefit ($N_{sa}=1$).

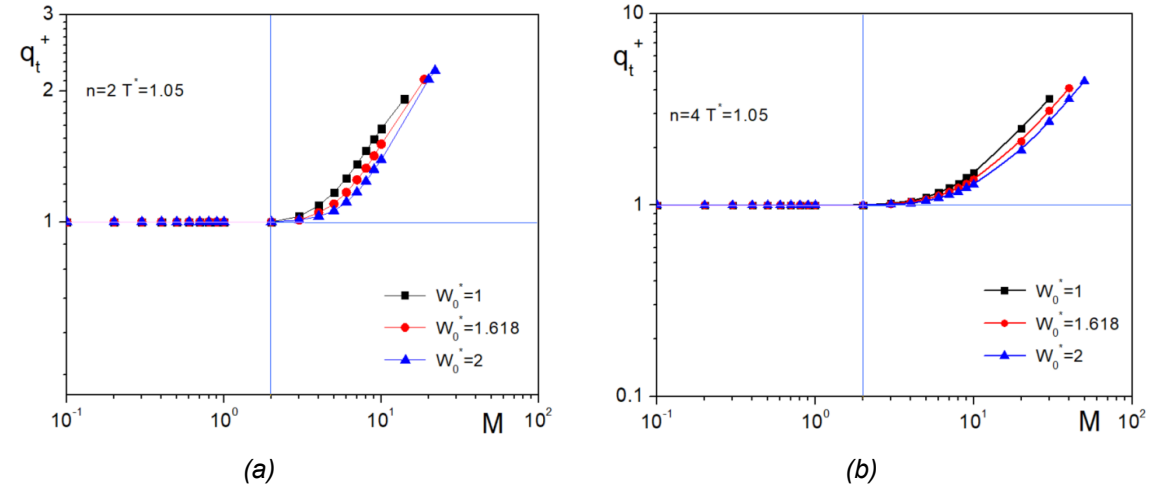

Figure 3. The variation of q_t^+ *with M and* W_o^*. *(a)* $n=2$, *(b)* $n=4$

Fig. 3 shows the variation of the heat flow ratio q_t^+ (first law benefit) with the dimensionless mass flow rate *M* and complexity n for two designed configurations studied. As seen, two different ranges of interest have been detected:

a) For mass flow rate $M\le 2$, the ratio $q_t^+=1$ means that the total heat flow does not increase despite the increase in the complexity, $n>0$, and M. In this regard, the case FG-1b [16] is available, namely, the objective is a maximum reduction of the driving temperature difference, $\Delta T_m^*<1$ or $N_{sa}<1$ which are interrelated. In this

case, the constraints are: fixed heat flow, $q_t^+ = 1$, fixed inlet mass flow *M*, fixed inlet temperature T_{in}, fixed channel wall temperatures T_w, and fixed heat transfer surface area A_w in the allocated area A.

b) for $M > 2$ the case FG-1a [16] is available, where the objective is increased heat flow, $q_t^+ > 1$, with constraints of fixed inlet fluid flow and channel wall temperatures, T_{in} and T_w, fixed mass flow rate M, fixed heat transfer surface area A_w, and reduction of the entropy generation, $N_{sa} \le 1$. It should be noted that the benefits can be calculated only if the two objectives $q_t^+ > 1$ and $N_{sa} \le 1$ are achieved.

(***Note:*** The end of each curve q_t^+ vs. M, according to complexity *n*, has been defined by the constraint $N_{sa} = 1$).

In the range $M > 2$, the first objective is an increase in the heat flow ratio, $q_t^+ > 1$, but the benefit could be indicated only if the constraint $N_{sa} \le 1$ is fulfilled. As seen from Fig. 3, q_t^+ increases with the increase in M and complexity n, reaching a limiting value for M. This maximum value of M has been limited by the constraint $N_{sa} = 1$.

For instance, for the tree-shaped design with $T^* = 1.05$ and $n = 2$ ($B = 10^{-11}$), Fig. 3a, the results calculated have shown that for $W_o^* = 1$, $1 < q_t^+ < 1.96$ in the range $2 < M \le 14.6$; for $W_o^* = 1.618$, $1 < q_t^+ < 2.26$ in the range $2 < M \le 20.0$, and for $W_o^* = 2.0$, $1 < q_t^+ < 2.3$ in the range $2 < M \le 23.5$.

Figure 3b shows the results for the tree-shaped design with a ratio $T^* = 1.05$ and $n = 4$ ($B = 10^{-11}$). As seen, for $W_o^* = 1$, $1 < q_t^+ < 3.59$ in the range $2 < M \le 30$; for $W_o^* = 1.618$, $1 < q_t^+ < 4.08$ in the range $2 < M \le 40.0$ and for $W_o^* = 2.0$, $1 < q_t^+ < 4.4$ in the range $2 < M \le 50$.

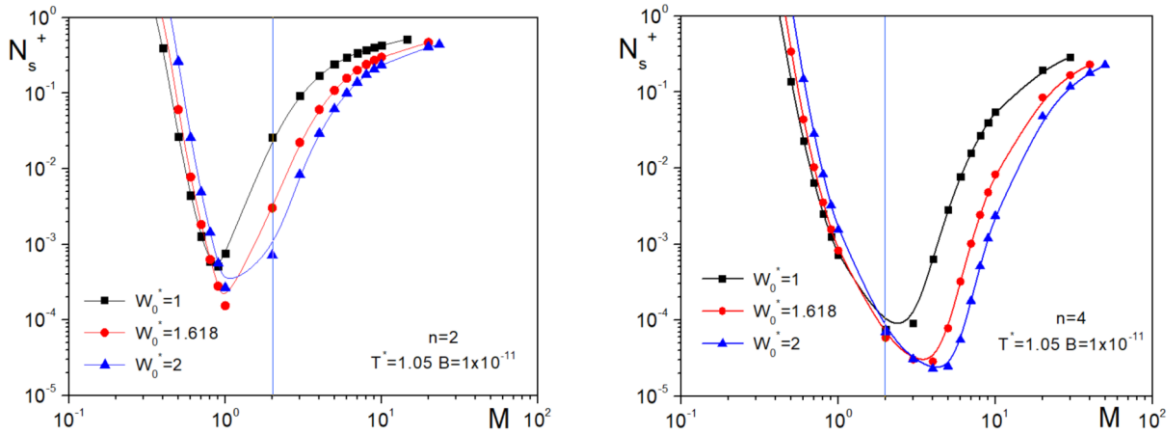

Figure 4. The variation of N_s^+ with M, W_o^*, (a) $n = 2$, (b) $n = 4$

It has to be noted that the value of q_t^+ depends only on the complexity *n* and *M*, whereas the value of N_{sa} depends on the values of T^*, B, n and M. For this reason, the ranges of M for which the requirement $N_{sa} \le 1$ is fulfilled depend on the values of T^*, and B chosen. In this regard, the foregoing analysis is valid only for these particular values of $T^* = 1.05$ and $B = 10^{-11}$.

Fig. 4 shows the variation of the general criteria N_s^+ with *M*, W_o^* and *B*, for $n = 2$ and $n = 4$. As seen, the general benefit increases when W_o^* and *n* increases. If $n = 4$, two objectives can be pursued: (a) the value of *M* for minimum entropy generation, $M = 4$ ($W_o^* = 2$) or (b) the value of *M* for maximum heat flow, $M = 50$.

Figures 5-7 present the variation of N_{sa}, q_t^+ and N_s^+ for $T^* = 1.4$. The comparison of the results obtained with those for $T^* = 1.05$ has revealed that the variation of T^* does not have any impact on the benefits.

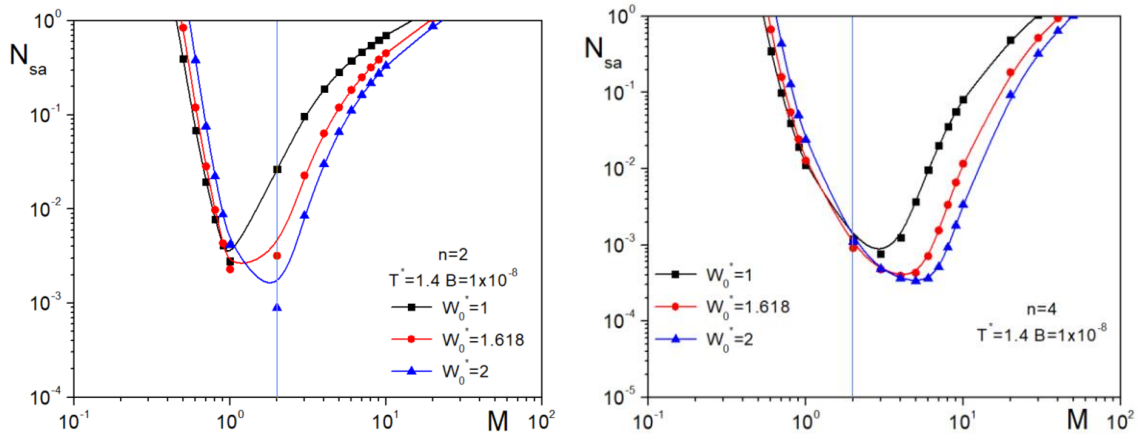

(a) (b)

Figure 5. The variation of N_{sa} with M and W_o^* (a) $n=2$, (b) $n=4$ ($B=10^{-8}$, $T^*=1.4$)

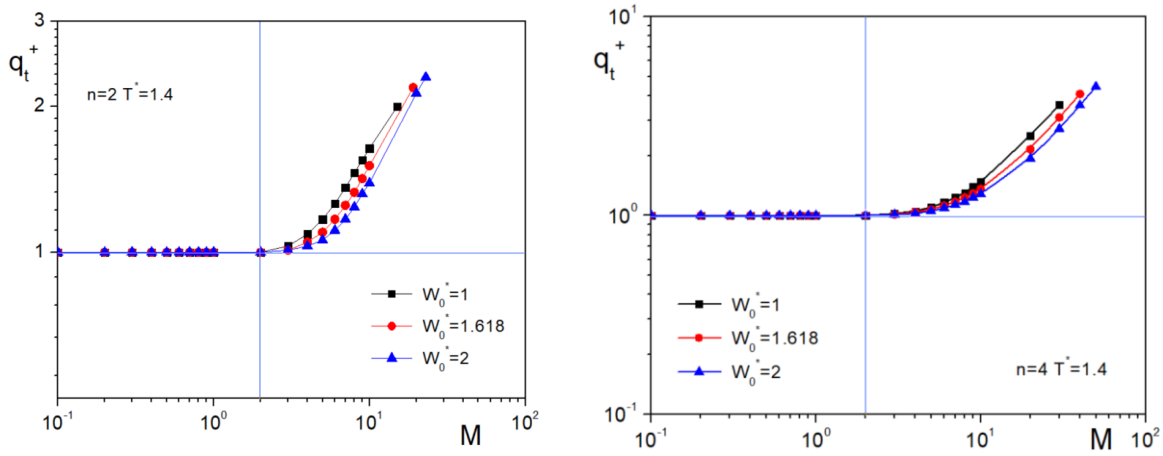

(a) (b)

Figure 6. The variation of q_t^+ with M and W_o^*. (a) $n=2$, (b) $n=4$

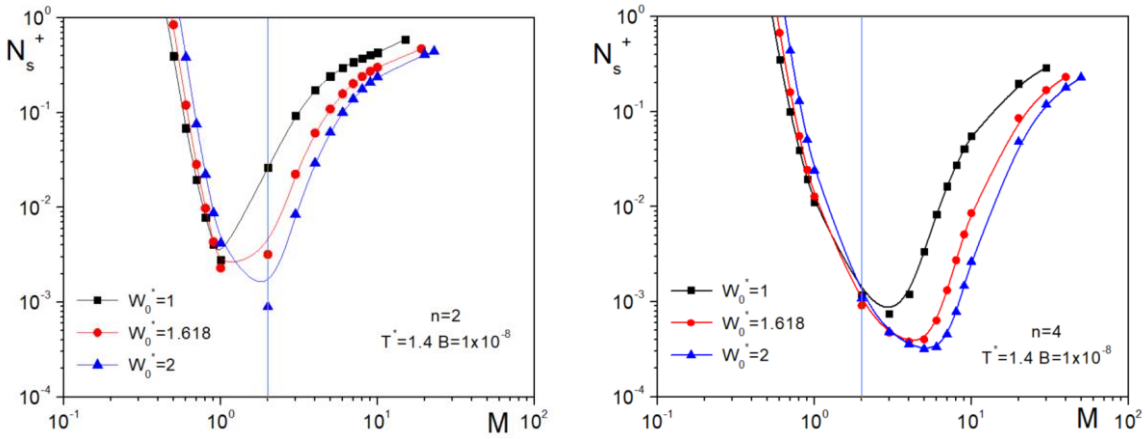

(a) (b)

Figure 7. The variation of N_s^+ with M, W_o^*, (a) $n=2$, (b) $n=4$

Conclusion

With this study, we try to encourage the use of several criteria as $q_t^+ > 1$, $N_{sa} \leq 1$ and the general criterion N_s^+ for assessing the benefits that tree-shaped heat exchangers can bring about in comparison with conventional heat exchangers with different structures like serpentine or banks of parallel tubes. These criteria arose from the first and second laws of thermodynamics, according to the objectives pursued and the constraints imposed. The comparison of the thermal performance characteristics of the tree-shaped design with serpentine tube design heat exchangers has been accomplished following these criteria.

Acknowledgments

This study has been supported by the European Regional Development Fund under the Operational Program "Scientific *Research, Innovation* and *Digitization* for *Smart Transformation* 2021-2027", Project CoC "Smart Mechatronics, Eco- and Energy Saving Systems and Technologies", BG16RFPR002-1.014-0005, Center of competence "Smart Mechatronics, Eco- and Energy Saving Systems and Technologies".

Nomenclature

A	area, (m^2)
A_w	heat transfer surface area, (m^2)
B	ratio
c_p	specific heat, ($J\,kg^{-1}K^{-1}$)
D	channel diameter, (m)
f	Fanning friction factor
h	heat transfer coefficient, ($W\,m^{-2}K^{-1}$)
k	thermal conductivity, ($W\,m^{-1}K^{-1}$)
L	length, (m)
M	dimensionless mass flow rate
$\dot{m}$	mass flow rate, ($kg\,s^{-1}$)
N_s	entropy generation ratio
N_{sa}	augmentation entropy generation number
N_s^+	performance evaluation criterion
Nu	Nusselt number
P	pumping power, (W)
Δp	pressure drop, (Pa)
n	number of pairing levels
$\dot{q}$	heat flow, (W)
$\dot{q}_{tot}$	total heat flow, (W)
$\tilde{q}$	dimensionless heat flow
q_t^+	heat flow ratio
$\dot{S}_{gen}$	entropy generation rate, ($W\,K^{-1}$)
$\tilde{S}_{gen}$	dimensionless entropy generation rate
T	temperature, (K)
T^*	(T_w / T_{in})
ΔT	temperature difference, (K)

Greek symbols

η	performance evaluation criterion
ϑ	temperature difference, (K)
ν	kinematic viscosity, ($m^2\,s^{-1}$)
ρ	density, ($kg\,m^{-3}$)

Subscripts

f	fluid
i	channel rank
in	inlet
m	mean
n	number of constructional levels
o	channel rank
out	outlet

References

[1] Manglik R.M., Bergles A.E., Heat transfer enhancement and pressure drop in viscous liquid flows in isothermal tubes with twisted-tape inserts. Wärme- und Stoffübertragung 1992;27:249-57.

[2] Webb R.L., Kim N.H., Principles of enhanced heat transfer. New York, USA: Taylor & Francis Group; 2005. p. 223-70.

[3] Saha S.K., Ranjan H., Emani M.S., Bharti A.K., Introduction to enhanced heat transfer. Cham, Switzerland: Springer; 2020. p. 35-64.

[4] Mousa M.H., Miljkovic N., Nawaz K., Review of heat transfer enhancement techniques for single-phase flows. Renewable and Sustainable Energy Reviews 2021;137:110566.

[5] García A., Vicente P.G., Viedma A., Experimental study of heat transfer enhancement with wire coil inserts in laminar-transitional-turbulent regimes at different Prandtl numbers. International Journal of Heat and Mass Transfer 2005;48:4640-51.

[6] García A., Solano J.P., Vicente P.G., Viedma A., Enhancement of laminar and transitional flow heat transfer in tubes by means of wire coil inserts. International Journal of Heat and Mass Transfer 2007;50:3176-89.

[7] Martínez D.S., García A., Solano J.P., Viedma A., Heat transfer enhancement of laminar and transitional Newtonian and non-Newtonian flows in tubes with wire coil inserts. International Journal of Heat and Mass Transfer 2014;76:540-48.

[8] Kumar A., Prasad B.N., Investigation of twisted tape inserted solar water heaters: heat transfer, friction factor and thermal performance results. Renewable Energy 2000;19:379-98.

[9] Zimparov V.D., Bonev P.J., Angelov M.S., Hristov J.Y., Benefits from the use of wire-coil inserts in water transitional and low turbulent flow: the influence of the wire-coil pitch. Thermal Science 2022;26(4B):3597-3604.

[10] Promvonge P., Thermal augmentation in circular tube with twisted tape and wire coil turbulators. Energy Conversion and Management 2008;49:2949-55.

[11] Zimparov V.D., Bonev P.J., Petkov V.M., Transitional heat transfer and pressure drop in plain horizontal tubes. International Review of Chemical Engineering 2015;7(2):37-44.

[12] Zimparov V.D., Bonev P.J., Petkov V.M., Benefits from the use of enhanced heat transfer surfaces in heat exchanger design: a critical review of performance evaluation. Journal of Enhanced Heat Transfer 2016;23(5):371-93.

[13] Zimparov V.D., Bonev P.J., Petkov V.M., Transitional heat transfer and pressure drop in plain horizontal tubes – revised study. International Review of Chemical Engineering 2017;9(1):1-7.

[14] Zimparov V.D., Penchev P.J., Bonev P.Y., Heat transfer enhancement with tube inserts: how can we define the best benefit? Thermal Science 2025;29(1B):509-20.

[15] Bejan A., Entropy generation through heat and fluid flow. New York, USA: John Wiley & Sons; 1982.